groups pointing in the same direction, should statistically be in 12.5% abundance, the (3,1) in 50%, the trans (2,2) in 12.5%, and the cis (2,2) in 25%. Thermal equilibration studies on various picket-fence porphyrin derivatives[28] show a number of cases where less of the (4,0) and more of the trans (2,2) derivative occur than expected statistically. Similarly, for a given porphyrin, Ni^{2+}, diacid, and free-base adducts interconvert ((4,0) → (3,1)) faster than do Zn^{2+}, Pd^{2+}, or Cu^{2+} derivatives, and the (4,0) free base shows atropisomerization of the resulting nickel complex under rather gentle nickel incorporation conditions. We do not know if H_2–TMPyP(2) interconverts upon equilibration with Pb^{2+}, as might be expected for a deformed Pb^{II}–P derivative. Equilibrium constants and rates of metal ion reactions with individual picket-fence porphyrin isomers have been studied. For copper[29] and zinc[30] kinetic work, the rate span is less than a factor of 6 among the four isomers and within a factor of 10 for equilibrium constants[30] of cadmium complexation in aqueous solution with water-soluble picket-fence porphyrins. The Pb^{2+}/H_2–TMPyP(2) reaction data presented are thus average values for the isomer distribution present.

For individuals with lead intoxication, large amounts of zinc protoporphyrin are found in the erythrocytes, presumably bound to the heme site of globin.[15] Pb^{2+}, Hg^{2+}, Mn^{2+}, and Zn^{2+} inhibit ferrochelatase,[31-33] the enzyme that incorporates Fe^{2+} into protoporphyrin IX. This enzyme can use Zn^{2+} and Co^{2+} as substrates in the absence of Fe^{2+}, and both Mn^{2+} and Zn^{2+} are competitive inhibitors[31,32] for Fe^{2+}. It has been speculated[15] that both enzymatic zinc chelatase activity[32] (which has a pH profile similar to those of Zn^{2+}/H_2–P reactions[34]) and nonenzymatic zinc chelation routes may be involved in the Zn–Proto formation in lead intoxication. On the basis of the present Zn^{2+}/Pb^{II}–P results, a lead-catalyzed route may also be operative. This notion, however, is tempered by the fact that in severe iron deficiency anemia, Zn–Proto is also formed, while for humans with inherited erythropoietic porphyria (a ferrochelatase deficiency), the unmetalated protoporphyrin IX is mainly produced.[15]

Acknowledgment. This work was supported by Howard University NIH Biomedical Research Grant 5-SO-6-RR-08016-9.

Registry No. H_2TMPyP(2), 59728-89-1; H_2TMPyP(4), 38673-65-3; H_2TAP, 69458-19-1; Pb, 7439-92-1; Zn, 7440-66-6; Co, 7440-48-4.

(28) Freitag, R. A.; Whitten, D. G. *J. Phys. Chem.* **1983**, *87*, 3918.
(29) Turay, J.; Hambright, P. *Inorg. Chim. Acta* **1981**, *53*, L147.
(30) Valiotti, A.; Adeyemo, A.; Williams, R. F. X.; Ricks, L.; North, J.; Hambright, P. *J. Inorg. Nucl. Chem.* **1981**, *43*, 2653.
(31) Dailey, H. A.; Fleming, J. E. *J. Biol. Chem.* **1983**, *258*, 11453.
(32) Camadro, J.-M.; Labbe, P. *Biochim. Biophys. Acta* **1982**, *707*, 280.
(33) Dailey, H. A.; Lascelles, J. *Arch. Biochem. Biophys.* **1974**, *160*, 523.
(34) Shamim, A.; Hambright, P. *Inorg. Chem.* **1983**, *22*, 694.

Contribution from the Section of Chemistry, Karl Marx University, DDR-7010 Leipzig, GDR

Single-Crystal EPR Spectra of $(n\text{-}Bu_4N)_2[^{63}Cu(dmit)_2]$

Joachim Stach, Reinhard Kirmse,* Wolfgang Dietzsch, Ruth-Maria Olk, and Eberhard Hoyer

Received February 17, 1984

Isotrithione-3,4-dithiolate (dmit; from the notation dimercaptoisotrithione used primarily) represents a new type of sulfur-rich dithiolene ligand forming covalent complexes with various metal ions.[1-3] Metal bis complexes of dithiolene ligands are known to show interesting electric and magnetic properties in dependence on the cations. Some of these compounds are of special interest for the preparation of linear-chain materials.[4-6] The EPR spectra—especially the single-crystal spectra—of the corresponding paramagnetic transition-metal complexes are characterized by very small line widths, allowing the detection of small ligand hyperfine interactions as shown for the Ni(III), Pd(III), and Pt(III) dmit complexes n-$Bu_4N[Ni(dmit)_2]$, n-$Bu_4N[Pd(dmit)_2]$, and n-$Bu_4N[Pt(dmit)_2]$.[7] The investigation of superhyperfine interactions (shfs) due to the interactions of the unpaired electron with ligand nuclei is useful for the characterization of the nature of the metal–ligand bonds because complete shfs data provide direct information about the molecular orbital of the unpaired electron and give a more detailed picture of the spin-density distribution in covalent complexes.

In this paper we report a detailed analysis of the ^{33}S superhyperfine interactions (^{33}S: natural abundance 0.74%, $I = {}^3/_2$) observed in the single-crystal EPR spectra of tetra-*n*-butylammonium bis(isotrithione-3,4-dithiolato)cuprate(II), $(n\text{-}Bu_4N)_2[Cu(dmit)_2]$ (**1**), diamagnetically diluted by the corresponding Ni(II) chelate.

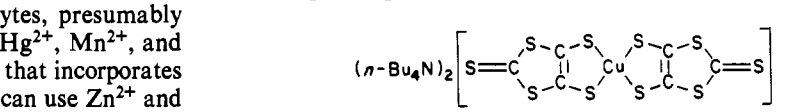

1

The experimental parameters will be compared with those obtained by Maki et al.[8] and Plumlee et al.[9] for $(n\text{-}Bu_4N)_2[Cu(mnt)_2]$ (mnt = *cis*-1,2-dicyanoethenedithiolate). Up to now ^{33}S hfs data have been detected only for a small number of complexes having a CuS_4 coordination sphere.[10-13]

Experimental Section

The ligand and the Cu(II) and Ni(II) complexes were prepared as described earlier by Steimecke et al.[1-3] For the preparation of $(n\text{-}Bu_4N)_2[^{63}Cu(dmit)_2]$, ^{63}Cu-enriched $CuCl_2 \cdot 2H_2O$ (97.8% ^{63}Cu, 2.2% ^{65}Cu) was used. Suitable single crystals containing about 0.5 mol % $(n\text{-}Bu_4N)_2[^{63}Cu(dmit)_2]$ in the corresponding Ni(II) complex could be grown by slow solvent evaporation from acetone/ethanol (20/1) solutions.

The EPR spectra were recorded on a Varian E-112 spectrometer in the X band at room temperature.

Results and Discussion

The structure of the host complex is known.[14] $(n\text{-}Bu_4N)_2[Ni(dmit)_2]$ crystallizes in the monoclinic space group $P2_1/c$, with two molecules per unit cell. The complex anion is nearly planar; Ni occupies an inversion center. As expected according to the structure of the Ni complex, the single-crystal

(1) Steimecke, G.; Kirmse, R.; Hoyer, E. *Z. Chem.* **1975**, *15*, 28.
(2) Steimecke, G. Ph.D. Thesis, Karl Marx University, Leipzig, 1977.
(3) Steimecke, G.; Sieler, J.; Kirmse, R.; Hoyer, E. *Phosphorus Sulfur* **1979**, *7*, 49.
(4) Siedle, A. R. *Ext. Linear Chain Compd.* **1982**, *2*, 469.
(5) Alcacer, L.; Novais, H. *Ext. Linear Chain Compd.* **1983**, *3*, 319.
(6) Kobayashi, A.; Sasaki, Y. *Bull. Chem. Soc. Jpn.* **1977**, *50*, 2650.
(7) Kirmse, R.; Stach, J.; Dietzsch, W.; Steimecke, G.; Hoyer, E. *Inorg. Chem.* **1980**, *19*, 2679.
(8) Maki, A. H.; Edelstein, N.; Davison, A.; Holm, R. H. *J. Am. Chem. Soc.* **1964**, *86*, 4580.
(9) Plumlee, K. W.; Hoffman, B. M.; Ibers, J. A.; Soos, Z. G. *J. Chem. Phys.* **1975**, *63*, 1926.
(10) Kirmse, R.; Stach, J.; Dietzsch, W.; Hoyer, E. *Inorg. Chim. Acta* **1978**, *26*, L53.
(11) Attanasio, D.; Keijzers, C. P.; Van den Berg, J. P.; De Boer, E. *Mol. Phys.* **1976**, *31*, 501.
(12) Kirmse, R.; Solovev, B. V. *J. Inorg. Nucl. Chem.* **1977**, *39*, 41.
(13) Stach, J.; Kirmse, R.; Dietzsch, W. *Inorg. Chim. Acta* **1979**, *36*, L395.
(14) Sjölin, L.; Lindqvist, O.; Sieler, J.; Steimecke, G.; Hoyer, E. *Acta Chem. Scand., Ser. A* **1979**, *A33*, 445.

0020-1669/84/1323-4779$01.50/0

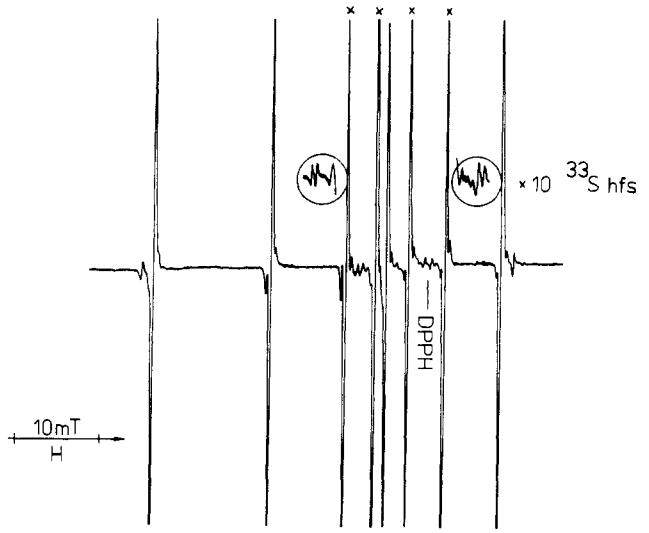

Figure 1. X-Band EPR spectrum of $(n\text{-Bu}_4N)_2[^{63}Cu(dmit)_2]$ in a $(n\text{-Bu}_4N)_2[Ni(dmit)_2]$ single crystal at $T = 298$ K. The magnetic field lies parallel to the coordination sphere for one (×) of the two magnetically nonequivalent Cu(II) complex anions in the unit cell.

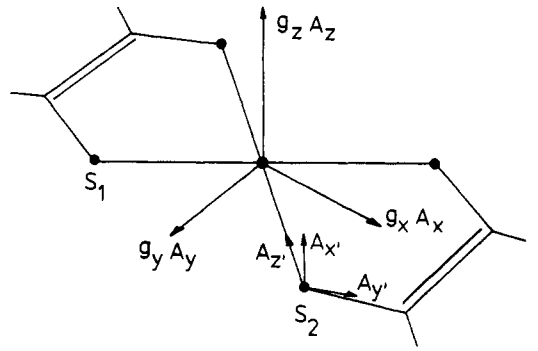

Figure 2. Orientations of the principal axes of the **g**, ^{63}Cu, and ^{33}S hfs tensors in $(n\text{-Bu}_4N)_2[Cu(dmit)_2]$.

EPR spectra of $[Cu/Ni(dmit)_2]^{2-}$ show the absorption peaks of two magnetically nonequivalent $[^{63}Cu(dmit)_2]^{2-}$ anions for a general direction of the magnetic field. Each Cu hfs line is flanked symmetrically by two sets of four ^{33}S shfs satellites. The intensity of the satellite lines is approximately 0.4% of that of the corresponding ^{63}Cu hfs signal. The observed satellites arise from complex molecules containing one ^{33}S donor atom only. Other cases in which more than one ^{33}S donor atom is present in $(n\text{-Bu}_4N)_2[Cu(dmit)_2]$ can be neglected due to the low natural abundance of ^{33}S. In addition to the ^{33}S shfs peaks in the spectra, each Cu hfs line is flanked by spin–flip satellites caused by weak dipolar interactions between the unpaired electron and the magnetic moment of neighbor protons. Moreover, Cu hfs transitions with $\Delta m_I \geq 1$ are to be seen in the spectra of the Cu complexes recorded for magnetic field orientations perpendicular to the molecular z axis. A representative spectrum is shown in Figure 1.

The EPR spectra were analyzed in terms of the spin Hamiltonian

$$\hat{H}_{sp} = \mu_B \mathbf{B}\cdot\mathbf{g}\cdot\hat{\mathbf{S}} + \hat{\mathbf{S}}\cdot\mathbf{A}^{Cu}\cdot\hat{\mathbf{I}}^{Cu} + \sum_{i=1}^{2}(\hat{\mathbf{S}}\cdot\mathbf{A}^{S_i}\cdot\hat{\mathbf{I}}^{S_i}) \qquad (1)$$

The third term in (1) describes the ^{33}S shfs interactions; the symbols used have their usual meaning. The principal values of the **g** tensor, the ^{63}Cu hfs tensor, and the ^{33}S shfs tensors measured for both sets of S atoms are listed in Table I; in addition, the corresponding values for $[Cu(mnt)_2]^{2-}$[8,9] are given for comparison. The directions of the principal axes of **g**, $\mathbf{A}^{Cu}$, and $\mathbf{A}^{S}$ in the molecular frame are shown in Figure 2. The directions of the maximum components of the ^{33}S shfs tensors, A_z^S, are found to be coincident with the directions of the Cu–S bonds.[10,11] The angle between the $A_z^{S_1}$ and $A_z^{S_2}$ components of the ^{33}S shfs tensors derived from the angular dependence measured in the xy plane of the complex molecule was found to be 90 ± 2°, which is in a good agreement with the S_1–Ni–S_2 angle of the host complex (88°). The third principal value, A_x^S, points in the direction of g_z and A_z^{Cu}.

Table I. EPR Parameters of $(n\text{-Bu}_4N)_2[^{63}Cu/Ni(dmit)_2]$ and $(n\text{-Bu}_4N)_2[^{63}Cu/Ni(mnt)_2]$[8,10] [a]

	$[Cu(dmit)_2]^{2-}$	$[Cu(mnt)_2]^{2-}$
g_z	2.101	2.086
g_y	2.027	2.026
g_x	2.025	2.023
g_{av}	2.051	2.045
A_z^{Cu}	−158.7	−161.1
A_y^{Cu}	−39.6	−39.0
A_x^{Cu}	−36.4	−38.0
A_{av}^{Cu}	−78.2	−79.4
$A_z^{S_1}$	22.4	22.0
$A_y^{S_1}$	9.9	7.9
$A_x^{S_1}$	10.5	9.4
$A_{av}^{S_1}$	14.3	13.1
$A_z^{S_2}$	21.2	21.4
$A_y^{S_2}$	10.0	7.6
$A_x^{S_2}$	10.5	9.4
$A_{av}^{S_2}$	13.9	12.8

[a] Hyperfine couplings in 10^{-4} cm^{-1}. Experimental errors: $g_{z,x} \pm 0.002$; $g_y \pm 0.003$; $A_{z,x}^{Cu} \pm 1.0$; $A_z^{Cu} \pm 2.0$; $A_z^S \pm 0.5$; $A_{x,y}^S \pm 1.0$.

The directions of the maximum components of the ^{33}S shfs tensors, A_z^S, are found to be coincident with the directions of the Cu–S bonds.[10,11] The angle between the $A_z^{S_1}$ and $A_z^{S_2}$ components of the ^{33}S shfs tensors derived from the angular dependence measured in the xy plane of the complex molecule was found to be 90 ± 2°, which is in a good agreement with the S_1–Ni–S_2 angle of the host complex (88°). The third principal value, A_x^S, points in the direction of g_z and A_z^{Cu}.

In the angular dependence of the ^{33}S shfs satellite spectra only two quartets are to be seen, indicating the presence of an inversion center. Therefore, the conclusion can be drawn that the structure of the incorporated Cu complex is in close accord with that of the Ni host complex, the structure of which is known.[14] The directions of the principal axes of the tensor parameters determined are in agreement with this conclusion.

The EPR parameters suggest a molecular orbital for the unpaired electron that can be written as

$$\psi_{B_{1g}} = \alpha|d_{xy}\rangle - (\alpha^{S_1}/2^{1/2})(-\sigma^1 + \sigma^3) - (\alpha^{S_2}/2^{1/2})(\sigma^2 - \sigma^4) \qquad (2)$$

where $\sigma^i = (1 - n^2)^{1/2}S^i \pm np^i$.

The MO coefficient α can be estimated from the values obtained for the **g** and $\mathbf{A}^{Cu}$ tensor components and the formulas given by McGarvey;[15] the ^{33}S data are correlated to the coefficients α^{S_1} and α^{S_2} and the hybridization degree "n" as described by us earlier.[12] The following values were obtained: $\alpha^2 = 0.56$, $\alpha^{S_1} = 0.31$, $\alpha^{S_2} = 0.29$, $n^{2(S_1)} = 0.95$, $n^{2(S_2)} = 0.95$. As found from the ^{33}S shfs data for other Cu(II) complexes having a planar CuS_4 coordination sphere, the covalency of the metal–ligand bond is very high. Compared with the corresponding values evaluated for $[Cu(mnt)_2]^{2-}$ ($\alpha^2 = 0.54$, $\alpha^{S_1} = 0.36$, $\alpha^{S_2} = 0.34$) the MO coefficients α^{S_1} and α^{S_2} of $[Cu(dmit)_2]^{2-}$ are remarkably smaller. The differences between the **g** and ^{63}Cu hfs tensor components of $[^{63}Cu/Ni(dmit)_2]^{2-}$ and $[^{63}Cu/Ni(mnt)_2]^{2-}$ are caused mainly by the excitation energies, which change in going from $[Cu(dmit)_2]^{2-}$ to $[Cu(mnt)_2]^{2-}$ as can be seen from the electronic spectra and different energies of the highest occupied orbital reflected by the electrochemical half-wave potentials.[2]

Registry No. 1, 72688-89-2.

(15) McGarvey, B. R. *Transition Met. Chem. (N.Y.)* **1966**, *3*, 89.